A robust post-insertion method for the preparation of targeted siRNA LNPs

L.E. Swart [a], C.A. Koekman [c], C.W. Seinen [c], H. Issa. [b], M. Rasouli. [a], R.M. Schiffelers [c], O. Heidenreich [a,d,*]

[a] *Princess Máxima Center for Pediatric Oncology, Utrecht, the Netherlands*
[b] *Department of Pediatrics, University Hospital Frankfurt, Goethe-University Frankfurt, Frankfurt (Main), Germany*
[c] *Clinical Chemistry and Haematology, University Medical Center Utrecht, Heidelberglaan 100, Utrecht 3584 CX, the Netherlands*
[d] *Wolfson Childhood Cancer Research Centre, Newcastle University, Newcastle upon Tyne, UK*

A R T I C L E   I N F O

A B S T R A C T

Targeted delivery of nucleic acids is gaining momentum due to improved efficacy, selectivity, increased circulation time and enhanced tissue retention in target cells. Using nucleic acid-based therapies previously undruggable targets have proven now to be amenable for treatment. Currently, several methods for preparing targeted or labelled delivery vehicles for nucleic acids are based on liposomal formulations. Lipid nanoparticles (LNPs) are structurally different from liposomes and these methods should therefore be evaluated before being translated to siRNA LNPs preparation protocols. Here, we describe a robust and facile method for the preparation of targeted or fluorescently labelled siRNA LNPs. Using a copper free strain-promoted azide-alkyne cycloaddition (SPAAC) we demonstrate that post-insertion of ligand-lipid conjugates into preformed LNPs is superior to direct-surface modification because it preserves the physicochemical parameters of the LNPs. We found that the time point of solvent removal by dialysis is critical and affects the hydrodynamic diameter of the LNPs; post-insertion after dialysis shows the smallest increase in hydrodynamic diameter and polydispersity index (PDI). The post-insertion of ligand-lipid conjugates also proceeded with rapid kinetics and high efficacy over a wide temperature range. Using this optimised protocol, we generated siRNA LNPs containing both targeting and fluorescent tracking ligands allowing us to monitor siRNA LNP uptake kinetics in dependence of the targeting ligand. In aggregate, we describe a robust approach for the generation of targeted and labelled siRNA LNPs that allows their controlled and facile decoration with ligand combinations.

1. Introduction

Lipid nanoparticles (LNPs) are the lead non-viral delivery systems currently used for nucleic acid-based therapeutics, including siRNA, mRNA or plasmid DNA that provide treatments for diseases by silencing pathogenic genes or by expressing therapeutic proteins. siRNA LNPs for example have the potential to selectively impair fusion genes that are exclusively expressed in cancer cells thus constituting tumour-specific targets (Issa et al., 2018b; Jyotsana et al., 2019; Mohanty et al., 2020). However, for realizing their full therapeutic potential, formulation optimization is still required.

Ligand-targeted carrier vehicles offer improved selectivity, increased circulation time and enhanced tissue retention in target cells *in vivo*. For liposomes, it has been shown that ligand-targeting increases binding and tissue retention thereby improving therapeutic efficacy associated with less off-target cytotoxicity compared to non-targeted liposomes (Debs et al., 1987; Goren et al., 2000; Goren et al., 1996; Iden and Allen, 2001; Lee and Low, 1995; Lopes de Menezes et al., 1998; Luciani et al., 2004; Moase et al., 2001; Tseng et al., 1999). In contrast, less is known on the *in vivo* behaviour and corresponding preparation of targeted LNPs. Labelling liposomes occurs via spontaneous insertion of a lipophilic tail of the ligand into their lipid bilayer. LNPs are lacking this bilayer, which

---

is likely to affect their insertion properties. Therefore, these processes need to be evaluated for LNPs (Kampel et al., 2021; Kedmi et al., 2018; Kulkarni et al., 2018; Leung et al., 2012; Veiga et al., 2019; Veiga et al., 2018; Viger-Gravel et al., 2018).

siRNA LNPs contain a largely hydrophobic core, consisting of inverted lipid micelles encapsulating oligonucleotides (Kulkarni et al., 2018; Leung et al., 2012; Viger-Gravel et al., 2018). This core needs to be maintained during the introduction of targeting ligands or antibodies as alterations might affect the LNP circulation time or efficacy by degrading the siRNA *in vivo*. The hydrodynamic diameter is important in this respect; with a "goldilocks zone" ranging from of 40 to 150 nm to avoid renal clearance and to maintain the ability to penetrate tissues and thereby more efficient uptake by target cells (Leung et al., 2012; Leung et al., 2015; Nakamura et al., 2020; Widmer et al., 2018).

For direct surface modification of liposomes, click chemistry approaches have been shown to be superior to Michael addition, due to better control over the coupling reaction and site-specific occurrence of reactive groups (Stefanetti et al., 2020; van Moorsel et al., 2019). For biological purposes bioorthogonal coupling, such as strain-promoted azide-alkyne cycloaddition (SPAAC) is favorable, by avoiding the toxic copper (I) as catalyst by a ring-strained alkyne (Oude Blenke et al., 2015).

The resulting conjugation product can be post-inserted into the nanoparticles. For liposomes the hydrophobic lipid tail of the conjugation product will preferentially insert into its lipid bilayer (Uster et al., 1996). This PEGylation approach allows the directed insertion on the particle surface in contrast to random insertion of PEG into the particle interior during self-assembly (Nakamura et al., 2012). Insertion into the bilayer of preformed liposomes has been shown to be a time and temperature-dependent transfer (Iden and Allen, 2001; Ishida et al., 1999; Yang et al., 2007).

We here describe a robust and facile method for decorating siRNA LNPs that combines a copper-free click approach with a post-insertion strategy (Cavalli et al., 2006; Frisch et al., 2010; Kumar et al., 2010; Leal et al., 2011; Sun et al., 2019). Using this approach, we demonstrate successful incorporation of both targeting and tracking ligands into siRNA LNPs. Post-insertion efficiently occurs at temperatures ranging from 25 °C to 55 °C within 30 min. We found hydrodynamic diameter and PDI of the targeted siRNA LNPs to be dependent on the time point of solvent removal as post-insertion after dialysis showed the smallest increase in these parameters, without leakage of the encapsulated cargo. Finally, we successfully used double-labelled siRNA LNPs for monitoring uptake kinetics in leukaemic cells, showing the possibility to decorate LNPs with different ligands. Taken together, this paper describes a robust approach for the generation of ligand targeted and fluorescent labelled siRNA LNPs that allows their controlled and facile decoration with ligand combinations.

2. Methods

2.1. Materials

Cholesterol, distearoylphosphatidylcholine (DSPC), 1,2-dimyristoyl-*sn*-glycero-3-methoxypolyethylene glycol-2000 (DMG-PEG$_{(2000)}$) and 1,2-distearoyl-*sn*-glycero-3-phosphoethanolamine-N-[amino(polyethylene glycol)-2000] salt (DSPE-PEG$_{(2000)}$) were ordered from Avanti Polar Lipids (Alabama, U.S.). The DNA barcode with the sequence A$_{PS}$G$_{PS}$A CGT GTG CTC TTC CGA TCT GAC ACA GTN NNN NNN AGA TCG GAA GAG CGT CGT G$_{PS}$T$_{PS}$ was ordered from Integrated DNA Technologies (Leuven, Belgium), where PS refers to phosphorothioate linkages. (6Z,9Z,28Z,31Z)-heptatriaconta-6,9,28,31-tetraen-19-yl-4-(dimethylamino)-butanoate (D$_{Lin}$-MC3-DMA) was ordered from DC Chemicals (Shanghai, China). Gamma-Irradiated 10 kDa Slide-A-Lyzers were ordered from Thermo Scientific (Waltham, Massachusetts, USA). The Quant-iT RiboGreen RNA Assay Kit was ordered from Thermo Scientific (Waltham, Massachusetts, USA). Small interfering ribonucleic

acid molecules (siRNA) (knockdown and mismatch control) were ordered from Axolabs (Kulmbach, Germany)(Heidenreich et al., 2003; Issa et al., 2018a; Issa et al., 2018c).

2.2. siRNA LNPs preparation

Lipids (D$_{Lin}$-MC3-DMA):DSPC:Cholesterol:DMG-PEG$_{(2000)}$:DSPE-PEG$_{(2000)}$-DBCO were dissolved in 100% ethanol at a molar ratio of 50:10:38.5:1.2:0.3. In the case of ligand post-insertion, this molar ratio was changed to 50:10:38.5:1.5:0.1 to accommodate additional PEG lipid-ligand conjugates (Jayaraman et al., 2012). PEG molar ratios between 1.2% and 1.5% were chosen under consideration of the requirements for circulation times and endosomal cargo release (Akinc et al., 2019; Braeckmans et al., 2010; Chen et al., 2016; Kim et al., 2021; Knop et al., 2010; Semple et al., 2005; Suk et al., 2016; Witzigmann et al., 2020).

siRNAs were dissolved in hybridization buffer (25 mM HEPES, 100 mM NaCl, pH 7.5) to a final concentration of 100 μM. For LNPs generation, siRNAs were diluted in 25 mM acetic acid (pH 4) to achieve an N/P ratio of 4. We encapsulated active siRNA targeting the RUNX1/ETO fusion site (siRE) and a mismatch control, where two nucleotides in the sequence have been swapped (siMM). siRNA LNPs were prepared in a NanoAssemblr Benchtop Instrument (Precision Nanosystems, Vancouver, Canada) with a total flow rate of 4 ml/min and a lipid:siRNA flowrate ratio of 1:3. Subsequently, ethanol was removed and the siRNA LNPs emulsion neutralized by overnight dialysis against phosphate-buffered saline (PBS) at 4 °C using Gamma-Irradiated 10 kDa MWCO Slide-A-Lyzers with PBS replacements after 1 and 2 h.

2.3. siRNA LNPs characterisation

#### 2.3.1. Particle size determination by dynamic light scattering (DLS)

The hydrodynamic diameter and polydispersity index (PDI) values were obtained from samples 10x diluted in Dulbecco's phosphate buffered saline (DPBS) using the Zetasizer Nano Series ZS (Malvern Instruments, Malvern Panalytical, Malvern, UK). Samples were measured in three runs over 5 min at 25 °C, 173° backscatter and the analysis model "General purpose" (attenuator at 7). Hydrodynamic diameters and PDI values were averaged from three runs.

2.3.2. Particle characterization by cryo-electron microscopy (cryoEM)

A drop of aqueous solution containing siRNA LNPs was added to fresh glow discharged Quantifoils (Au 200 mesh from with a layer of holy carbon R3.5/1) and incubated for at least 5 min in a humidified environment. After incubation the Quantifoils were blotted for 5 s and subsequently vitrified in liquid ethane with a Vitrobot Mark VI (Field Electron and Ion Company, Hillsboro, USA). The resulting Quantifoils were stored in liquid nitrogen until imaging. Images were acquired with a FEI Tecnai G2 20 TWIN LaB6 emitter high voltage range 20–200 kV transmission electron microscope at spotsize 5. To that end, the vitrified Quantifoils were loaded in a liquid nitrogen pre-cooled Gatan 70° tilt cryo-transfer system and inserted in the microscope. Samples images were acquired by the bottom mounted FEI High-Sensitive (HS) Eagle CCD 4 k camera (Cell-Bio Biotechnology Co. Ltd., Switzerland) at 29,000-fold magnification.

2.3.3. siRNA concentration and encapsulation efficiency

The siRNA concentration was determined using the Quant-iT Ribo-Green RNA Assay Kit following standard protocol. In brief, LNPs were incubated with 0.5% (*v/v*) Triton X-100 (total siRNA concentration) or with DPBS (free siRNA) at 37° for 15 min. Encapsulation efficiency was then determined by the quotient of [total siRNA concentration - free siRNA]/[total siRNA concentration] $\times$ 100.
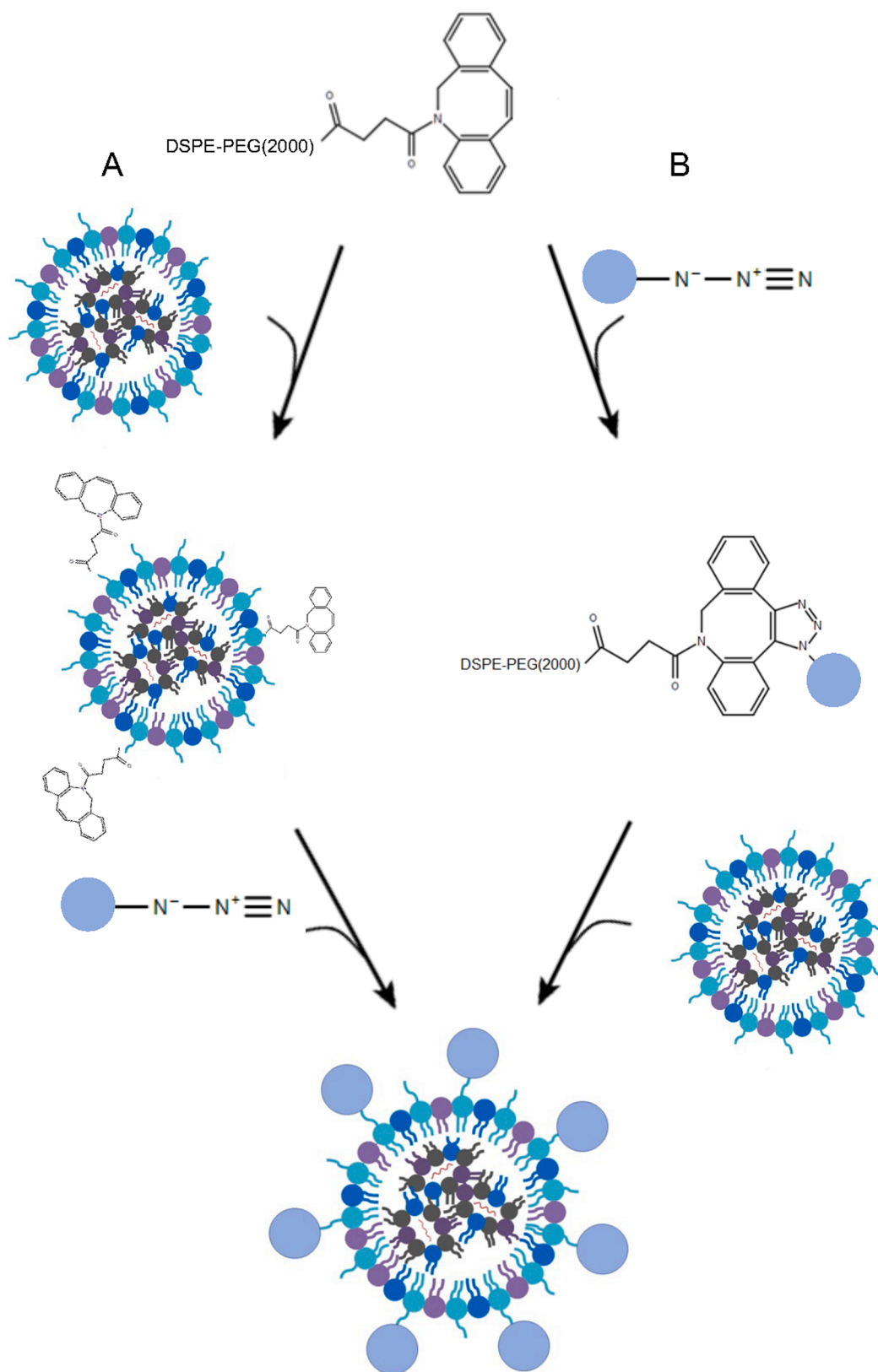
Fig. 1. Investigated methods for preparation of targeted siRNA LNPs. (A) Preformed siRNA LNPs containing 0.1% molar ratio DBCO-DSPE-PEG$_{(2000)}$ are incubated with an azide-containing component in a molar ratio of DBCO:azide of 3:1. Under physiological conditions these components then form a conjugate on the surface of the LNPs. (B) The azide-containing component and DBCO-DSPE-PEG$_{(2000)}$ are first conjugated together and consequently post-inserted into preformed siRNA LNPs before or after dialysis.

2.4. Click chemistry conjugation

Sulfo-Cy3-azide or (2-[4-(3-(o-Tolyl)ureido)-phenyl]-acetyl)-L-leucyl-L-aspartyl-L-valinyl-L-propargylglcine-azide (LDV-azide) were first conjugated to the ring-constrained alkyne DBCO, that was bound to DSPE-PEG$_{(2000)}$. The higher transition energy of this ring-constrained alkyne leads to spontaneous reaction with an azide and has already been used to label liposomes (Oude Blenke et al., 2015). Sulfo-Cy3-azide dissolved in H$_2$O or LDV-ligand-azide dissolved in DMSO:H$_2$O 3:2 were added to DSPE-PEG$_{(2000)}$-DBCO to a molar ratio of 1:3. The mixture was
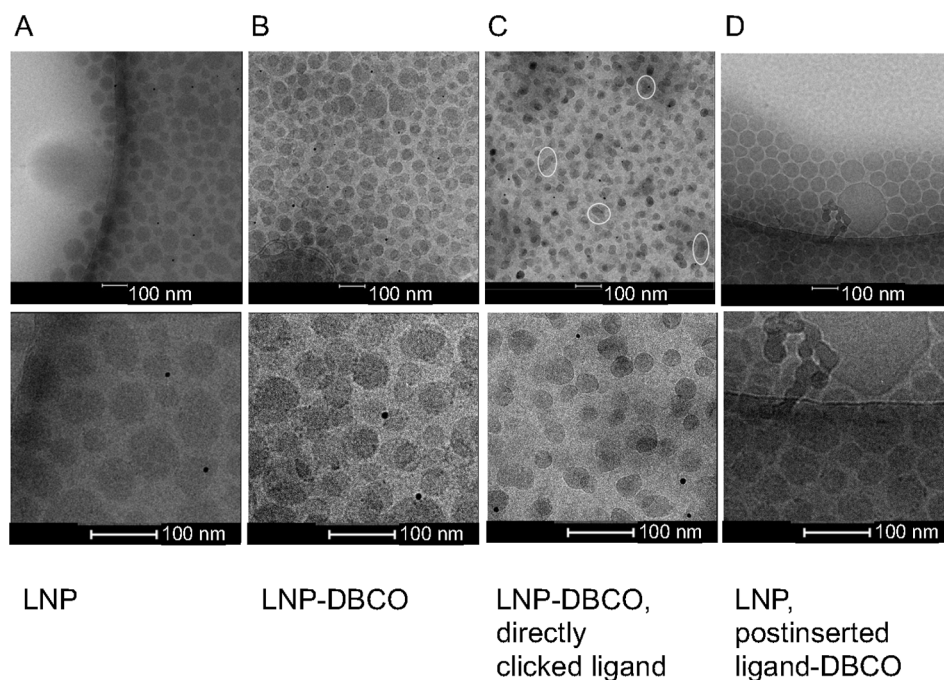
Fig. 2. Cryo EM analysis of siRNA LNP morphology. (A) Image of siRNA LNPs containing 1.5% DMG-PEG$_{(2000)}$. (B) siRNA LNPs containing 1.5% DMG-PEG$_{(2000)}$ and 0.1% molar ratio DSPE-PEG$_{(2000)}$-DBCO added to the microfluidic mixture. (C) siRNA LNPs with LDV-ligand-azide directly clicked to DBCO present on the surface of siRNA LNPs. White circles highlight fused siRNA LNPs. (D) siRNA LNPs with 0.1% molar ratio DSPE-PEG$_{(2000)}$-triazole-ligand post-inserted after dialysis. The bottom panel shows 3 times enlarged details of the top images.

incubated overnight at room temperature protected from the dark. The resulting conjugation product was kept for up to 7 days at 4 °C till post-insertion reaction.

2.5. Labelling of siRNA LNPs

Current models suggest that post-insertion of PEG takes place via micelle intermediates from which monomers are released (Iden and Allen, 2001; Ishida et al., 1999). The post-insertion process can occur because of the hydrophobic lipid tail of the PEG-lipid micelles that preferentially inserts into the lipid bilayer.(Uster et al., 1996) If not stated otherwise, siRNA LNPs were incubated with DSPE-PEG$_{(2000)}$-DBCO (conjugated to the LDV-ligand or Cy3-fluorophore and unconjugated) before or after dialysis for 2 h at 45 °C. Following post-insertion, the siRNA LNPs were transferred to Gamma-Irradiated Slide-A-Lyzers with 10 kDa MWCO and dialysed overnight against PBS, with exception off the direct addition sample. After 12 h the siRNA LNPs were removed from the dialysis membrane and hydrodynamic diameter and PDI were measured as described previously using DLS. Samples were kept for up to 7 days at 4 °C till measurement.

2.6. Co-elution on the AKTA pure

Co-elution experiments were done using an AKTA pure with a fraction collector F9-C (GE Healthcare Life Sciences, Eindhoven, Nederland) and a 1 ml sample loop for application of the siRNA LNPs solutions. The separation of the siRNA LNPs from the micelles was performed using a Sepharose CL-4B column (self-made, volume 30 ml, max pressure 0.4 ml/min). The method-based unit was column volumes (CV) and the default flow rate was set to 0.5 ml/min with flow control to avoid overpressure. The running conditions were inlet A1 that contained 0.22 μm filtered PBS (pH = 7.4). The run started with 1 CV of inlet A1 washing step (flow rate 0.5 ml/min), followed by an equilibration step, where the column was washed with inlet A1 until the UV signal was stabilized. 500–600 μl of the siRNA LNPs were mixed gently and directly applied to the column using 1 ml capillary loop (sample application). The bound molecules were eluted by applying 1 CV of A1 with automatic peak fractionation to collect the 0.5 ml fractions in a deep-well 96 well plate. After the run the column was washed once with 1 CV A1 and

consequently washed with 1 CV 0.22 μm filtered 20% ethanol solution.

2.6.1. Absorbance of the collected fractions on the Spectramax iD3

150 μl of the fractions were transferred to a black flat-bottom 96-well plate and absorbance (Cy3: λ (550 nm) - λ (590 nm); Cy5: λ (633 nm - λ (670 nm)) was measured using the Spectramax iD3 (Molecular Devices, San Jose, California, USA).

2.7. General cell culture

Kasumi-1 cells were cultured in RPMI1640 containing 10% fetal bovine serum (FBS), while SKNO-1 cells were cultured in RPMI1640 supplemented with 20% FBS and 10 ng/ml granulocyte–macrophage colony-stimulating factor (GM-CSF) at 37 °C in a humidified atmosphere containing 5% CO$_2$. Cells were regularly authenticated and tested for mycoplasma.

2.8. Flow cytometry to measure uptake of fluorescent labelled-LNPs in cell lines

Cells were seeded at $5*10^5$ cells/ml and 2 ml/well in a 24-well plate. If not otherwise, Cy3-labelled siRNA LNPs with and without LDV-ligand were added to the wells to a final concentration of 2 μg/ml followed by incubation for up to 24 h at 37 °C and 5% CO$_2$. At indicated time-points 100 μl of the cell suspension were transferred to a V-bottom 96-well plate and washed once in FACS buffer containing sterile PBS with 0.025% BSA, 0.02% NaN$_3$ and 1% FBS. After centrifugation for 4 min at ×350 g, cell pellets were resuspended in 150 μl FACS buffer. To remove membrane bound siRNA LNPs the cells were sequentially washed with acetic acid buffer (0.5 M NaCl, 0.2 M acetic acid, pH 4) and FACS buffer. Upon fixation in 150 or 100 μl 2% paraformaldehyde (PFA) in PBS, plates were kept for up to 7 days at 4 °C in the dark until measurement.

Cy3 fluorescence was measured with Cytoflex LX (Beckman Coulter, Brea, California, United States of America) in the Y585-PE channel and 130 μl or 90 μl sample volume was acquired. Data were analyzed with FlowJo.v10.7.1. Normalised siRNA LNP uptake was calculated by subtracting the median autofluorescence from the median Cy3 signal from the samples.

Table 1

DLS measurement of siRNA LNPs. The letters correspond with the CryoEM figure shown in Fig. 1. Mean ± SD (n = 3).

Sample	Hydrodynamic diameter (nm)	PDI
A	63 ± 9	0.09 ± 0.05
B	110 ± 4	0.18 ± 0.01
C	153 ± 9	0.25 ± 0.004
D	93 ± 23	0.16 ± 0.04

2.9. RNA isolation, cDNA synthesis and qPCR to determine RUNX1/ETO knockdown with Cy3-labelled siRNA LNPs

At 24 h cells were harvested and washed twice with sterile PBS (centrifugation for 5 min at 350*g*) and consequently lysed using RLT buffer from the RNeasy Mini Kit (Qiagen, California, USA). RNA was isolated following supplier's protocol. 500 ng cDNA was prepared using the RevertAid H Minus First Strand cDNA Synthesis Kit (Thermo Scientific, Waltham, Massachusetts) following supplier's protocol.

Primers sequences are listed in Table S1. cDNA samples were diluted to 15 ng input/well prior qPCR analysis with RNAse-free H_2O. Samples were measured in triplicate, with 2 μl of diluted cDNA or RNase free water added to 8 μl of the qPCR reaction mix, containing primers and the SsoAdvanced™ Universal SYBR® Green Supermix (Bio-rad). *GAPDH* and *TBP* were used as house-keeping genes.

qPCR was done using CFX384 thermal cycler (Bio-Rad Laboratories, United States of America) with PCR cycling conditions as follows: a polymerase activation and DNA denaturation step for 30 s at 95 °C, followed by 35 cycles of denaturation (95 °C for 15 s), annealing and extension (60 °C for 30 s), followed by melting curve analysis (65 °C for 5 s, 95 °C).

3. Results

3.1. Post-insertion of linked lipid acceptor molecules conserves the siRNA LNPs morphology

We asked how direct ligand decoration of LNPs by click reaction affects LNPs structure and size in comparison to post-insertion. To that end, we prepared siRNA LNPs containing 1.5% DMG-PEG$_{(2000)}$ and 0.1% DSPE-PEG$_{(2000)}$-DBCO followed by directly conjugating LDV-ligand-azide to the DBCO groups on the surface of preformed siRNA LNPs (Fig. 1A). Alternatively, we generated siRNA LNPs containing 1.5% DMG-PEG$_{(2000)}$, where we post-inserted DSPE-PEG$_{(2000)}$-triazole-ligand at a 0.1% molar ratio (Fig. 1B). CryoEM imaging showed that siRNA LNPs containing 1.5% DMG-PEG$_{(2000)}$ have a hydrophobic solid core and are uniformly sized. The hydrodynamic diameter was around 60 nm as measured by DLS (Fig. 2A and Table 1, sample A).

Direct addition of DSPE-PEG$_{(2000)}$-DBCO to the lipid mixture to a molar ratio of 0.1% resulted in twofold increase in the hydrodynamic diameter and PDI (Table 1, second entry), but preserved the solid core structure of the siRNA LNPs (Fig. 2B). This substantial size increase

could be caused by an inwards orientation of the DBCO groups when not bound to an azide, as previously reported for PEG during self-assembly (Uster et al., 1996). Conjugation of the ligand-azide to the surface DBCO resulted in micellar fragments with increased hydrodynamic diameter and PDI indicating a disruption of the spherical structure of the siRNA LNPs (Table 1, third entry, Fig. 2C). Moreover, we observed larger, multi lamellar particles, possibly resulting from fusion of several siRNA LNPs. In contrast, post-insertion of the DSPE-PEG$_{(2000)}$-triazole-ligand preserved the spherical shape and solid core of the siRNA LNPs as shown in Fig. 2D. Importantly, this was associated with an increase in hydrodynamic diameter by 50% (Table 1, entries 2 and 4). This behaviour was neither ligand nor cargo dependent: We obtained comparable results for decorated with variable domains of heavy-chain-only antibodies (VHHs) ligand LNPs containing a DNA barcode (Fig. S1, Table S2). While direct surface clicking resulted in large micellar fragments and increased the hydrodynamic diameter and PDI, post-insertion of DSPE-PEG$_{(2000)}$-triazole-VHH preserved LNP structure as determined by cryo EM and caused a < 50% increase in size.

3.2. Post-insertion after dialysis preserves hydrodynamic diameter of siRNA LNPs

We next investigated if we should perform the post-insertion before or after dialysis. The post-preparative dialysis step of siRNA LNPs neutralises the surface charge and causes particle maturation by stabilizing the assembled lipid structure by removal of residual ethanol (Kulkarni et al., 2018). To investigate the most optimal post-insertion strategy for preparing targeted siRNA LNPs, we prepared siRNA LNPs containing DMG-PEG$_{(2000)}$ at molar ratios of 1.2% and 1.5% followed by post-insertion of DSPE-PEG$_{(2000)}$-DBCO (conjugated to the LDV-ligand and unconjugated) to molar ratios of 0.3% or 0.1%, respectively (Fig. 1B). Importantly, post-insertion did not result in leakage of the siRNA during the post-insertion procedure (Fig. S2). DLS measurements showed that both inclusion of unconjugated DBCO into to lipid mixture and post-insertion of the LDV-ligand-conjugate prior to dialysis increased the hydrodynamic diameter more than twofold. In the case of 1.2% DMG-PEG$_{(2000)}$ it also doubled the PDI of the LNPs (Braeckmans et al., 2010; Kim et al., 2021; Knop et al., 2010; Suk et al., 2016). Post-insertion of the LDV conjugate after dialysis increased the size of LNPs containing 1.5% PEG by 10–30%, but did not increase the PDI as judged by DLS and cryoEM measurements (Table 2, entries 1 and 5 comparing to 4 and 8). We therefore decided to continue with siRNA LNPs containing 1.5% DMG-PEG$_{(2000)}$ because of their higher homogeneity and anticipated stability for *in vivo* applications (Chen et al., 2014; Chen et al., 2016; Ryals et al., 2020). In conclusion, post-insertion of the LDV-ligand conjugate after dialysis had the least impact on particle size, homogeneity and encapsulated cargo.

Table 2

Impact of post insertion or direct conjugation on hydrodynamic diameter (nm) and PDI of Cy3-labelled siRNA LNPs. The siRNA LNPs (1) were prepared with 1.5% molar ratio DMG-PEG$_{(2000)}$ and 0.1% DSPE-PEG$_{(2000)}$-DBCO (conjugated to the LDV-ligand and non-conjugated) was added prior to and after dialysis. The siRNA LNPs (2) were prepared with 1.2% molar ratio DMG-PEG$_{(2000)}$ and 0.3% DSPE-PEG$_{(2000)}$-DBCO (conjugated to the LDV-ligand and non-conjugated) was added before and after dialysis. Mean ± SD (n = 3). *, $p < 0.05$; **, $p < 0.01$; ***, $p < 0.001$; two-tailed Student's *t*-test.

Sample	%DMG-PEG$_{(2000)}$	%DSPE-PEG$_{(2000)}$-DBCO	%DSPE-PEG conjugate	Post-inserted	Size (nm)	PDI	p value
LNP 1.0	1.5	0	0	n/a	66 ± 8	0.147 ± 0.076	0.13
LNP 1.1	1.5	0.1	0	before dialysis	117 ± 30	0.147 ± 0.051	0.33
LNP 1.2	1.5	0	0.1	before dialysis	124 ± 10	0.140 ± 0.052	0.099
LNP 1.3	1.5	0	0.1	after dialysis	93 ± 23	0.161 ± 0.038	na
LNP 2.0	1.2	0	0	n/a	73 ± 10	0.136 ± 0.044	0.22
LNP 2.1	1.2	0.3	0	before dialysis	137 ± 19	0.181 ± 0.102	0.008
LNP 2.2	1.2	0	0.3	before dialysis	172 ± 4	0.201 ± 0.045	<0.0001
LNP 2.3	1.2	0	0.3	after dialysis	82 ± 4	0.246 ± 0.053	na

Table 3

Impact of post-insertion reaction temperature on hydrodynamic diameter (nm) and PDI of Cy3-labelled siRNA LNPs. Temperature dependence of the post-insertion strategy the hydrodynamic diameter (nm) and PDI of the different batches of siRNA LNPs were measured via DLS. The LNPs (1) were prepared with 1.5% molar ratio DMG-PEG$_{(2000)}$ and 0.1% DSPE-PEG$_{(2000)}$-triazole-Cy3 and were subjected to post-insertion at different temperatures for 2 h. The table displays the mean and range (n = 2).

Sample	t (h)	T (°C)	Size (nm) [range]	PDI [range]
LNP 1.0	n/a	n/a	78 [65, 90]	0.205 [0.144, 0.266]
LNP 1.1	2	25	79 [77, 80]	0.197 [0.144, 0.249]
LNP 1.2	2	35	79 [74, 84]	0.227 [0.172, 0.281]
LNP 1.3	2	45	64 [60, 68]	0.197 [0.174, 0.219]
LNP 1.4	2	55	77 [68, 85]	0.180 [0.17, 0.189]

3.3. Post-insertion of Cy3 conjugated DBCO into siRNA LNPs efficiently occurs in a wide temperature range

For liposomes, the efficiency of the post-insertion reaction is temperature dependent and influenced by the phase transition temperature of the lipids (Iden and Allen, 2001; Ishida et al., 1999; Yang et al., 2007). To investigate if this parameter influences post-insertion into siRNA LNPs we incubated pre-formed Cy5-siRNA LNPs with 0.1% molar ratio DSPE-PEG$_{(2000)}$-triazole-Cy3 at temperatures ranging from 25 °C to 55 °C for 2 h. This range was chosen based on the phase transition temperature of the lipids and the thermal stability of the siRNA double-strand. DLS measured hydrodynamic diameters in the range of 64 nm to 79 nm (Table 3, all entries) for all temperatures examined. Compared to preformed LNPs (size 78 nm, Table 3, entry 1) this can be considered as no increase in size. Also the PDI was not affected by the post-insertion of Cy3-conjugate across the whole temperature range examined.

Current models suggest that post-insertion of PEG takes place via micelle intermediates (Iden and Allen, 2001; Ishida et al., 1999). To determine the fractions of post-inserted and free micelles we performed co-elution experiments on a Sepharose CL-4B column, which should separate Cy5-siRNA LNPs from Cy3-micelle-intermediates. Notably, for all investigated temperatures the Cy5 dye peak completely overlapped with the Cy3 dye peak with comparable median fluorescence intensities (MFIs) demonstrating a complete post-insertion of Cy3 conjugate (Figs. 3 and S3) as measured by the absorbance of the Cy5 and Cy3 dye. Here, the fast protein liquid chromatography (FPLC) elution profiles again showed in all conditions complete overlap of the Cy5 dye peak with the Cy3 dye peak. Thus, post-insertion efficiently occurs within a temperature range from 25 °C to 55 °C. We therefore chose for all subsequent post-insertion experiments 45 °C as the standard temperature.

3.4. Post-insertion of Cy3-conjugated DBCO into siRNA LNPs occurs until 3.5% total PEG ratio

Liposomal post-insertion has been reported to reach a plateau at 10% total PEG depending on the initial lipid composition (Mare et al., 2018). To determine the maximum amount of PEG that can be post-inserted into 1.5% preformed siRNA LNPs we incubated pre-formed Cy5-siRNA LNPs with different molar ratios of DSPE-PEG$_{(2000)}$-triazole-Cy3 ranging from 0.5% to 4% at 45 °C for 30 min. Monitoring the reaction progress by FPLC revealed a rapid completion of post-insertion for up to 2% PEG (Fig. S4A). PEG concentrations higher than 2% (corresponding to more than 3.5% total molar ratio of PEG in the LNPs) resulted in the formation of free DSPE-PEG$_{(2000)}$-triazole-Cy3 micelles and incomplete post-insertion associated with LNP disruption. This was confirmed by DLS, where larger particles (mean 218 nm and mean 565 nm) were detected
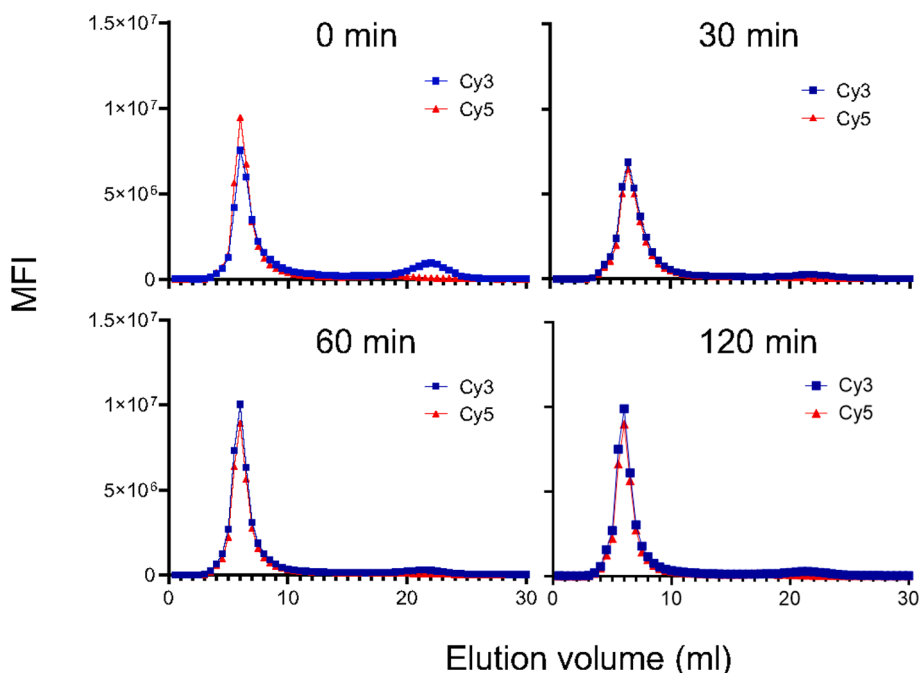
Table 4

Impact of post-insertion of increasing PEG concentrations on hydrodynamic diameter (nm) and PDI of Cy3-labelled siRNA LNPs. The siRNA LNPs were prepared with 1.5% molar ratio DMG-PEG$_{(2000)}$ and 0.5%, 1%, 1.5%, 2%, 3% or 4% DSPE-PEG$_{(2000)}$-DBCO (conjugated to Cy3-azide). The table displays the mean ± SD (n = 3).

Sample	% PEG	Total % PEG	Size (nm)	PDI
1	0.5	2.0	58 ± 1	0.151 ± 0.059
2	1.0	2.5	61 ± 2	0.165 ± 0.030
3	1.5	3.0	61 ± 4	0.132 ± 0.006
4	2.0	3.5	64 ± 6	0.158 ± 0.070
5	3.0	4.5	215 ± 269	0.249 ± 0.106
6	4.0	5.5	565 ± 164	0.310 ± 0.128
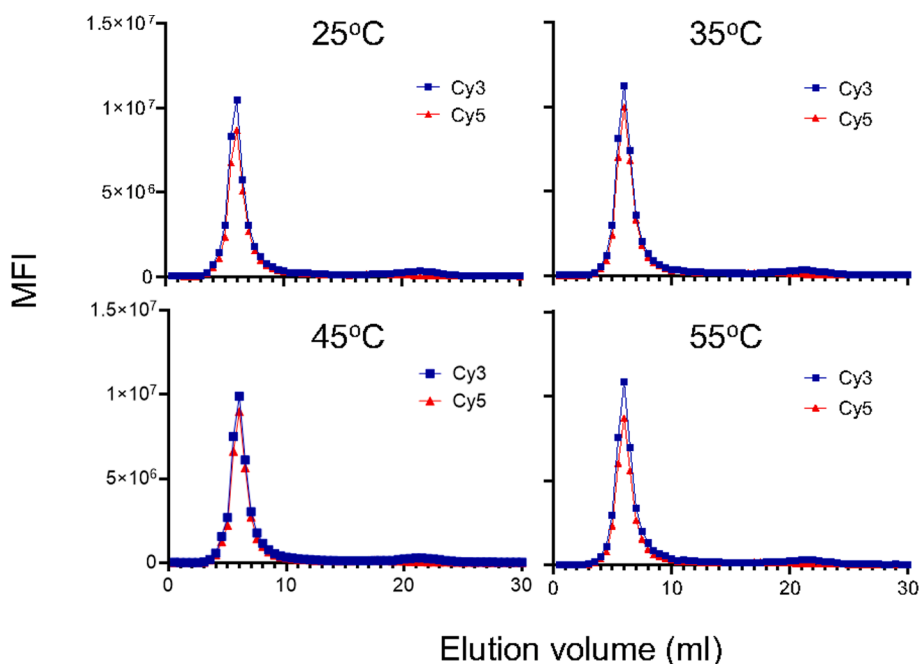
Fig. 3. Temperature independence of post-insertion reaction. Graphs showing FPLC elution profiles of LNPs containing Cy5-siRNA after incubation with DSPE-PEG$_{(2000)}$-triazole-Cy3 for 2 h at different temperatures. Reaction temperatures are indicated at the top of each graph.

Fig. 4. Post-insertion reaction kinetics. Graphs showing FPLC elution profiles of LNPs containing Cy5-siRNA after incubation with DSPE-PEG$_{(2000)}$-triazole-Cy3 at 45 °C for 0–2 h. Reaction times are indicated at the top of each graph.

Table 5
Impact of post-insertion reaction time on hydrodynamic diameter (nm) and PDI of Cy3-labelled siRNA LNPs. Kinetics of the post-insertion strategy the hydrodynamic diameter (nm) and PDI of the different batches of siRNA LNPs were measured via DLS. The siRNA LNPs (2) were prepared with 1.5% molar ratio DMG-PEG$_{(2000)}$ and 0.1% DSPE-PEG$_{(2000)}$-triazole-Cy3 was post-inserted at 45 °C for different incubation times. The table displays the mean and range (n = 2).

Sample	t (h)	T (°C)	Size (nm) [range]	PDI [range]
LNP 2.0	n/a	n/a	78 [65, 90]	0.205 [0.144, 0.266]
LNP 2.1	0	n/a	n/a	n/a
LNP 2.2	0.5	45	75 [65, 85]	0.151 [0.142, 0.160]
LNP 2.3	1	45	75 [66, 83]	0.144 [0.129, 0.159]
LNP 2.4	2	45	64 [60, 68]	0.197 [0.174, 0.219]

for 3% and 4% post-inserted PEG (Table 4 and Fig. S4B). In conclusion, PEG post-insertion reaches a plateau in between 2% and 3% based on the elution profiles and the DLS measurements confirming that ratios of 0.1% and 0.3% conjugated PEG$_{(2000)}$ result in proper post-insertion.

*3.5. Post-insertion of Cy3-conjugated DBCO into siRNA LNPs is a rapid reaction.*

Liposomal post-insertion efficiency has been previously reported to be time dependent, with optimal times in the 2–4 h region when incubated at elevated temperatures above the phase transition temperature of the lipids (Iden and Allen, 2001; Ishida et al., 1999). To evaluate the effect of this parameter on siRNA LNPs post-insertion we incubated preformed Cy5-siRNA LNPs with 0.1% DSPE-PEG$_{(2000)}$-triazole-Cy3 at 45 °C for 0–2 h. Monitoring the reaction progress by FPLC revealed a rapid completion of post-insertion at 45 °C (Fig. 4). Only for the 0 h time-point a smaller Cy3 peak can was detected indicating the presence of free DSPE-PEG$_{(2000)}$-triazole-Cy3 and incomplete post-insertion. However, since sample injection and column acquisition took 10 min, we therefore concluded that post-insertion is completed within this period. The same result was obtained when we repeated the co-elution of time-dependent post-inserted Cy5-siRNA LNPs (Fig. S5). The FPLC

elution profiles showed again overlap of the Cy5 peak with the Cy3 peak in all conditions indicating high efficiency of the post-insertion reaction. Moreover, we did not observe significant differences between the hydrodynamic diameter and PDI over 2 h of incubation which means preservation of the physicochemical parameters of the preformed siRNA LNPs (Table 5). Post-insertion of DSPE-PEG$_{(2000)}$-triazole-Cy3 into siRNA LNPs occurs rapidly with completion of the process within 30 min. Based on these results, we suggest that DSPE-PEG$_{(2000)}$-triazole-ligand conjugates should be post-inserted after dialysis into the preformed siRNA LNP at 45 °C for 30 min at molar ratios between 0.1% and 0.3% (Fig. 5).

3.6. Cy3-labeled siRNA LNPs have similar effect as compared to unlabeled siRNA LNPs

Next, we investigated whether post-insertion of a fluorescent label affects the biological activity of siRNA LNPs. To that end, we examined the siRNA-mediated knockdown of the leukaemic fusion gene *RUNX1/ETO* that is expressed in the AML cell lines Kasumi-1 and SKNO-1 (Rothdiener et al., 2010). We generated LNPs encapsulating either an siRNA targeting the *RUNX1/ETO* fusion transcript (siRE-mod) or a mismatch control with two exchanged nucleotides (siMM-mod). We then treated Kasumi-1 or SKNO-1 cells with the siRNA LNPs with and without post-inserted Cy3 conjugates at a dose of 2 μg/ml for 24 h. As shown in Fig. 6A, both Cy3-labelled and non-labelled LNPsiRE-mod yielded twofold knockdown of the *RUNX1/ETO* fusion transcript when compared with the mismatch control demonstrating that siRNA LNPs prepared via the described post-insertion method do not have altered efficacy *in vitro*.

Finally, we examined the possibility of inserting two different functional groups conjugated to DSPE-PEG$_{(2000)}$-DBCO into siRNA LNPs to monitor the cellular uptake. To that end we used DSPE-PEG$_{(2000)}$-triazole-Cy3 as an easy to monitor second ligand as an alternative to the commonly used Dil, DIO, DiD dyes for labelling LNPs. We combined Cy3 with an LDV-conjugate targeting VLA-4, which is widely expressed on haematopoietic cells. Uptake assays by FACS *in vitro* demonstrated that VLA-4-targeting resulted in a significantly improved uptake when compared to non-targeted siRNA LNPs, which translated into an
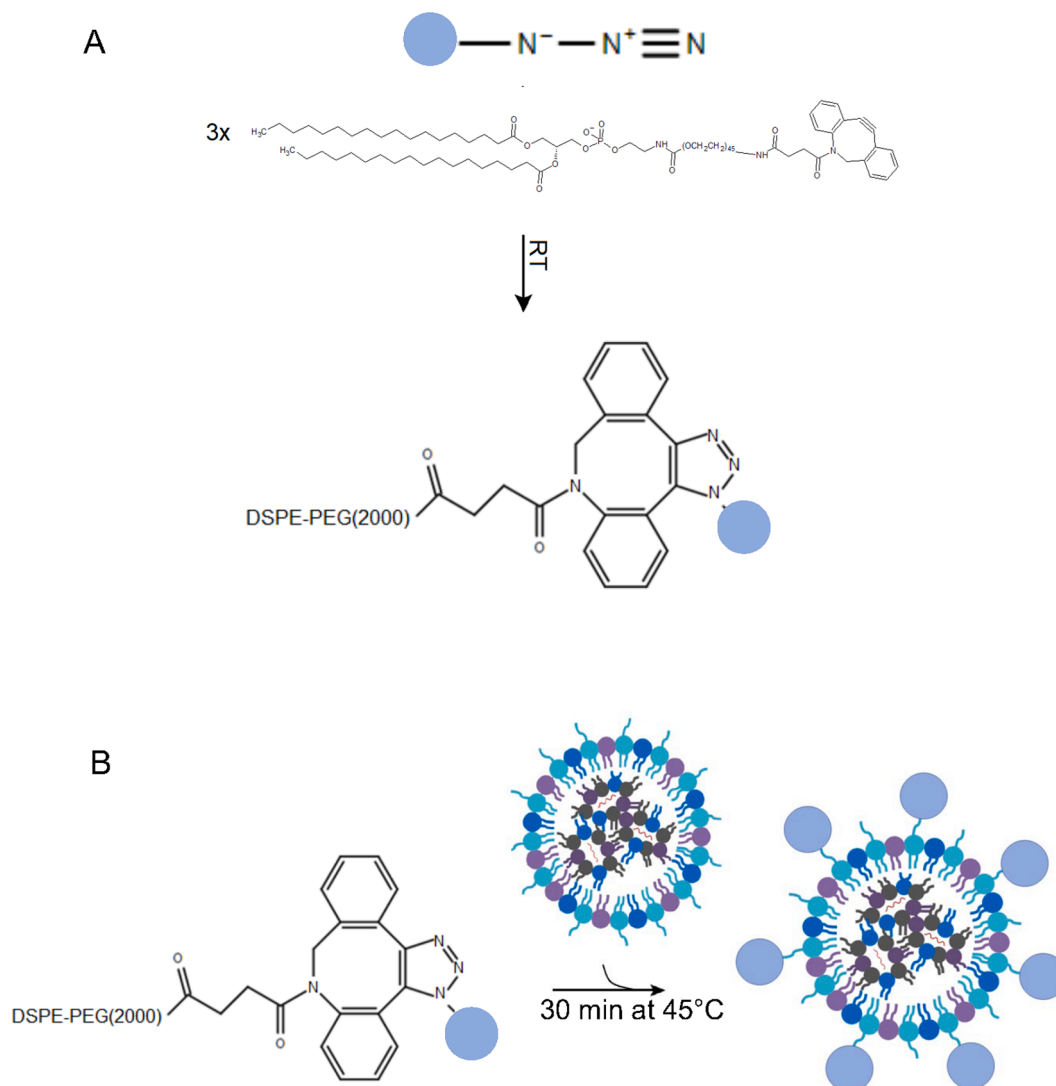
Fig. 5. Optimised procedure for siRNA LNP generation. (A) Strain-promoted azide-alkyne addition (SPAAC) using the restraint alkyne DSPE-PEG$_{(2000)}$-DBCO and azide bound to dye or ligand. Under physiological conditions at RT these two components form a conjugate that connects the LNPsiRNA to the alkyne following a copper-free click chemistry approach. The molar ratio of DBCO:azide is 3:1. (B) The SPAAC conjugate is post-inserted into preformed siRNA LNPs at molar ratio of 0.1% DSPE-PEG$_{(2000)}$-triazole-ligand. The reaction is carried out at 45 °C for 2 h.

accelerated knockdown of *RUNX1/RUNX1T1* transcript by the targeted LNP formulation (Fig. 6B, C). This finding demonstrates the feasibility of our post-insertion approach to generate siRNA LNPs with multiple functionalities for tracking and cell interactions and the possibility to double label via this post-insertion strategy. This approach could be useful for reaching difficult targets, where binding to two surface receptors is required for functional uptake.

4. Discussion

Targeted siRNA LNPs are a promising approach for the therapeutic intervention with pathologic gene expression. However, there is a scarcity of optimised preparation protocols and a lack of insight into important parameters. Here, we explored a copper-free click-chemistry approach combined with a post-dialysis PEGylation step to prepare targeted siRNA LNPs. We found that this method efficiently inserts PEG and therewith linked ligands into LNPs, independent of the cargo and linker, without significantly affecting physicochemical parameters and the encapsulated cargo of the preformed LNPs. Such modified LNPs show superior biologicial activity both in terms of uptake and knock-down kinetics in AML cells.

Post-insertion of conjugated PEG into preformed 1.2% PEG siRNA LNPs resulted in an increase in PDI, whereas this did not occur when post-insertion into 1.5% PEG siRNA LNPs took place. LNPs with lower PEG contents have been previously found to be less stable and to correlate with a higher aggregation tendency of particles (Braeckmans et al., 2010; Kim et al., 2021; Knop et al., 2010; Suk et al., 2016). Consequently, preformed LNPs containing 1.2% PEG are less stable than those with 1.5% PEG and are therefore more likely to aggregate during the post-insertion process.

The post-insertion kinetics of conjugated PEG is surprising, given that liposomal PEG post-insertion has been found to be a time and temperature dependent process. Incubation times of up to 48 h are reported and influenced mainly by the incubation temperature (Cosco et al., 2017; Eliasen et al., 2019; Ishida et al., 1999; Moreira et al., 2002). Moreover, short incubation times do not seem to result in complete and homogeneous post-insertion for liposomes (Eliasen et al., 2019). In contrast, we found that PEGylation of siRNA LNPs by post-insertion is complete within 30 min over a wider temperature range. Furthermore, while liposomes routinely contain PEG concentrations of 10% and higher, only up to 2% of conjugated PEG could be efficiently post-inserted into preformed 1.5% PEG LNPs. Finally, an important finding
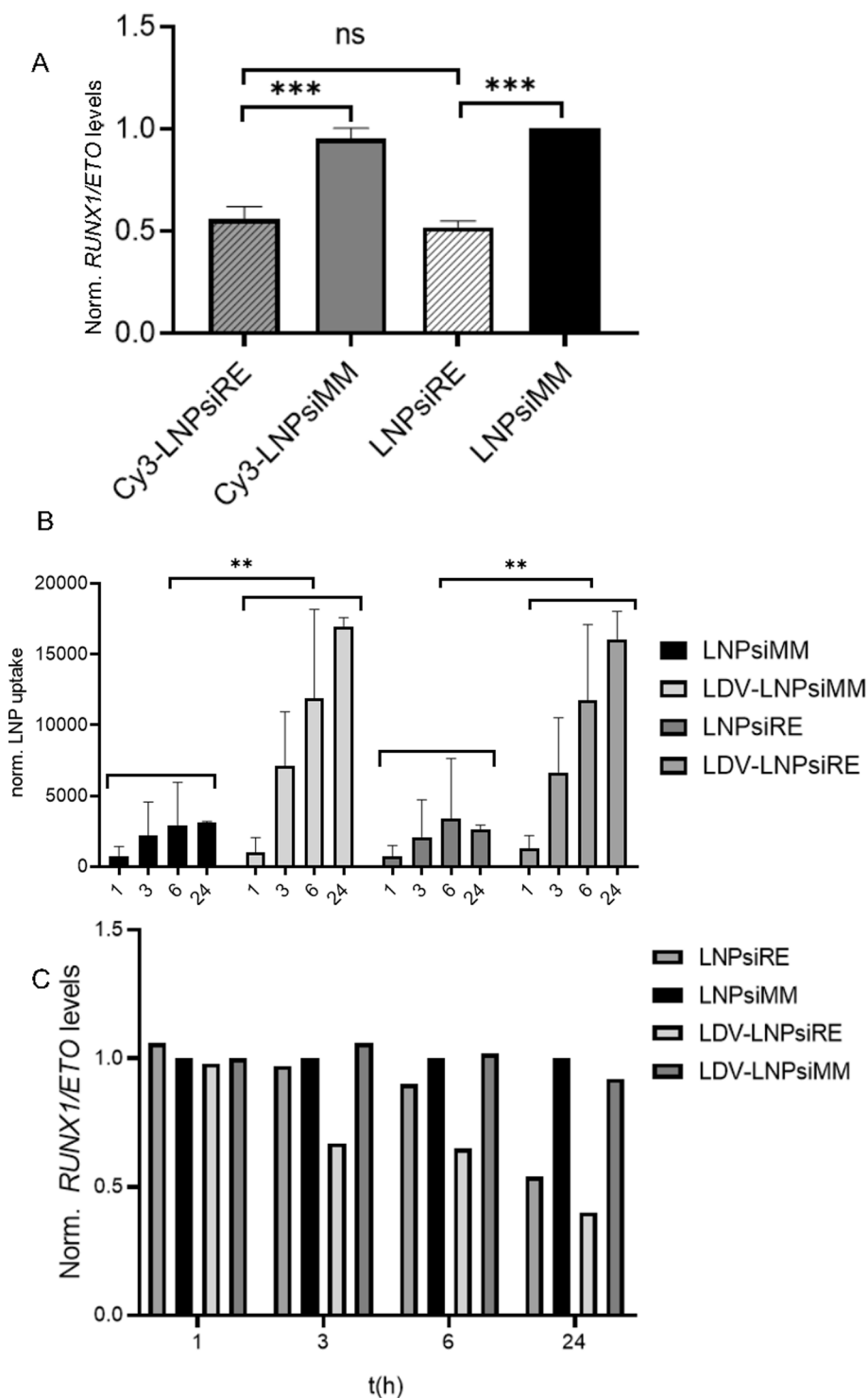
Fig. 6. Activity of Cy3-containing siRNA LNPs in leukaemic cells and uptake kinetics of ligand-Cy3-containing siRNA LNPs in leukaemic cells. (A) Reduction of *RUNX1/ETO* fusion transcript of siRNA LNPs with and without post-inserted Cy3 label. Kasumi-1 and SKNO-1 cells were incubated for 24 h with indicated siRNA LNPs followed by analysis of RNA transcript reduction by qPCR. *$P < 0.05$, **$P < 0.01$, ***$P < 0.001$, two-tailed Student's *t*-test. (B) Graph showing uptake of fluorescent-labelled siRNA LNPs with and without post-inserted LDV-ligand by Kasumi-1 and SKNO-1 cells. Mean $\pm$ SD (n = 4). *$P < 0.05$, **$P < 0.01$, ***$P < 0.001$, two-way ANOVA. siRE, siRNA targeting the fusion site of the *RUNX1/ETO* transcript; siMM, mismatch control siRNA. (C) Reduction of *RUNX1/ETO* fusion transcript of siRNA LNPs with and without post-inserted LDV-ligand. SKNO-1 cells were incubated for 1, 3, 6 or 24 h with 0.1 μg/ml indicated siRNA LNPs followed by analysis of RNA transcript reduction by qPCR. siRE, siRNA targeting the fusion site of the *RUNX1/ETO* transcript; siMM, mismatch control siRNA. All samples are normalised against the C_t value of the LNPsiMM.

of this study was that the time point of the post-insertion, i.e., before or after dialysis, has a strong impact on particle size and homogeneity. This has not been seen for liposomes (Takeuchi et al., 2019). These findings strongly suggest that both kinetics and thermodynamics of post-insertion can be different between liposomes and LNPs and that procedures cannot be easily transferred from one particle class to the other.

To conclude, targeted and fluorescently labelled siRNA LNPs can be prepared following a facile and robust method using a copper-free click chemistry approach. The post-insertion of the conjugated DBCO was superior to a direct click-mediated conjugation on the surface of the

siRNA LNPs. The time point of solvent removal was critical, as the hydrodynamic diameter and PDI of the siRNA LNPs were preserved best when the post-insertion was done after the dialysis. The post-insertion process was temperature independent over a temperature range from 25 °C to 55 °C and was completed within 30 min. Post-insertion of a fluorescent label did not compromise knockdown efficacy of siRNA LNPs and could be used for generating LNPs with multiple functionalities.

Funding

CRediT authorship contribution statement

L.E. Swart: methodology, investigation, formal analysis, writing—original draft, All authors have read and agreed to the published version of the manuscript. **C.A. Koekman:** investigation, writing—review and editing, All authors have read and agreed to the published version of the manuscript. **C.W. Seinen:** investigation, writing—review and editing, All authors have read and agreed to the published version of the manuscript. **H. Issa:** methodology, writing—review and editing, All authors have read and agreed to the published version of the manuscript. **M. Rasouli:** methodology, writing—review and editing, All authors have read and agreed to the published version of the manuscript. **R.M. Schiffelers:** Conceptualization, writing—review and editing, supervision, All authors have read and agreed to the published version of the manuscript. **O. Heidenreich:** Conceptualization, formal analysis, funding acquisition, writing—original draft, supervision, All authors have read and agreed to the published version of the manuscript.

Declaration of Competing Interest

The authors declare the following financial interests/personal relationships which may be considered as potential competing interests: Olaf Heidenreich has patent Targeted lipid nanoparticle formulations pending to Princess Maxima Center for Pediatric Oncology.

Acknowledgements

Appendix A. Supplementary material

Supplementary data to this article can be found online at https://doi.org/10.1016/j.ijpharm.2022.121741.

References

Akinc, A., Maier, M.A., Manoharan, M., Fitzgerald, K., Jayaraman, M., Barros, S., Ansell, S., Du, X., Hope, M.J., Madden, T.D., Mui, B.L., Semple, S.C., Tam, Y.K., Ciufolini, M., Witzigmann, D., Kulkarni, J.A., van der Meel, R., Cullis, P.R., 2019. The Onpattro story and the clinical translation of nanomedicines containing nucleic acid-based drugs. Nat. Nanotechnol. 14 (12), 1084–1087.

Braeckmans, K., Buyens, K., Bouquet, W., Vervaet, C., Joye, P., Vos, F.D., Plawinski, L., Doeuvre, L., Angles-Cano, E., Sanders, N.N., Demeester, J.o., Smedt, S.C.D., 2010. Sizing nanomatter in biological fluids by fluorescence single particle tracking. Nano Lett. 10 (11), 4435–4442.

Cavalli, S., Tipton, A.R., Overhand, M., Kros, A., 2006. The chemical modification of liposome surfaces via a copper-mediated [3 + 2] azide-alkyne cycloaddition monitored by a colorimetric assay. Chem. Commun. (Camb.) 3193–3195.

Chen, S., Tam, Y.Y.C., Lin, P.J.C., Leung, A.K.K., Tam, Y.K., Cullis, P.R., 2014. Development of lipid nanoparticle formulations of siRNA for hepatocyte gene silencing following subcutaneous administration. J. Control. Release 196, 106–112.

Chen, S., Tam, Y.Y.C., Lin, P.J.C., Sung, M.M.H., Tam, Y.K., Cullis, P.R., 2016. Influence of particle size on the in vivo potency of lipid nanoparticle formulations of siRNA. J. Control. Release 235, 236–244.

Cosco, D., Tsapis, N., Nascimento, T.L., Fresta, M., Chapron, D., Taverna, M., Arpicco, S., Fattal, E., 2017. Polysaccharide-coated liposomes by post-insertion of a hyaluronan-lipid conjugate. Colloids Surf B Biointerf. 158, 119–126.

Debs, R.J., Heath, T.D., Papahadjopoulos, D., 1987. Targeting of anti-Thy 1.1 monoclonal antibody conjugated liposomes in Thy 1.1 mice after intravenous administration. BBA 901, 183–190.

Eliasen, R., Andresen, T.L., Larsen, J.B., 2019. PEG-Lipid Post Insertion into Drug Delivery Liposomes Quantified at the Single Liposome Level. Adv. Mater. Interf. 6 (9), 1801807. https://doi.org/10.1002/admi.v6.910.1002/admi.201801807.

Frisch, B., Hassane, F.S., Schuber, F., 2010. Conjugation of ligands to the surface of preformed liposomes by click chemistry. Methods Mol. Biol. 605, 267–277.

Goren, D., Horowitz, A.T., Tzemach, D., Tarshish, M., Zalipsky, S., Gabizon, A., 2000. Nuclear delivery of doxorubicin via folate-targeted liposomes with bypass of multidrug-resistance efflux pump. Clin. Cancer Res. 6, 1949–1957.

Goren, D., Horowitz, A.T., Zalipsky, S., Woodle, M.C., Yarden, Y., Gabizon, A., 1996. Targeting of stealth liposomes to erbB-2 (Her/2) receptor: in vitro and in vivo studies. Br. J. Cancer 74 (11), 1749–1756.

Heidenreich, O., Krauter, J., Riehle, H., Hadwiger, P., John, M., Heil, G., Vornlocher, H.P., Nordheim, A., 2003. AML1/MTG8 oncogene suppression by small interfering RNAs supports myeloid differentiation of t(8;21)-positive leukemic cells. Blood 101, 3157–3163.

Iden, D.L., Allen, T.M., 2001. In vitro and in vivo comparison of immunoliposomes made by conventional coupling techniques with those made by a new post-insertion approach. Biochimica et Biophysica Acta (BBA) – Biomembranes 1513 (2), 207–216.

Ishida, T., Iden, D.L., Allen, T.M., 1999. A combinatorial approach to producing sterically stabilized (Stealth) immunoliposomal drugs. FEBS Lett. 460, 129–133.

Issa, H., Blair, H., Dal Porto, A., Jyotsana, N., Heuser, M., Heidenreich, O., 2018a. Therapeutic targeting of the leukaemic fusion gene RUNX1/ETO. Klin. Padiatr. 230, 168.

Issa, H., Blair, H., Jyotsana, N., Heuser, M., Heidenreich, O., 2018b. Therapeutic targeting of the leukaemic fusion gene RUNX1/ETO VIA RNAI. EHA Library. Issa H. Jun 15 2018; 215835, EHA.

Issa, H., Blair, H., Jyotsana, N., Heuser, M., Heidenreich, O., 2018c. Therapeutic targeting of the leukemic fusion gene RUNX1/ETO via RNAi. Hemasphere 2, 52.

Jayaraman, M., Ansell, S.M., Mui, B.L., Tam, Y.K., Chen, J., Du, X., Butler, D., Eltepu, L., Matsuda, S., Narayanannair, J.K., Rajeev, K.G., Hafez, I.M., Akinc, A., Maier, M.A., Tracy, M.A., Cullis, P.R., Madden, T.D., Manoharan, M., Hope, M.J., 2012. Maximizing the potency of siRNA lipid nanoparticles for hepatic gene silencing in vivo. Angew. Chem. Int. Ed. Engl. 51, 8529–8533.

Jyotsana, N., Sharma, A., Chaturvedi, A., Budida, R., Scherr, M., Kuchenbauer, F., Lindner, R., Noyan, F., Sühs, K.-W., Stangel, M., Grote-Koska, D., Brand, K., Vornlocher, H.-P., Eder, M., Thol, F., Ganser, A., Humphries, R.K., Ramsay, E., Cullis, P., Heuser, M., 2019. Lipid nanoparticle-mediated siRNA delivery for safe targeting of human CML in vivo. Ann. Hematol. 98 (8), 1905–1918.

Kampel, L., Goldsmith, M., Ramishetti, S., Veiga, N., Rosenblum, D., Gutkin, A., Chatterjee, S., Penn, M., Lerman, G., Peer, D., Muhanna, N., 2021. Therapeutic inhibitory RNA in head and neck cancer via functional targeted lipid nanoparticles. J. Control. Release 337, 378–389.

Kedmi, R., Veiga, N., Ramishetti, S., Goldsmith, M., Rosenblum, D., Dammes, N., Hazan-Halevy, I., Nahary, L., Leviatan-Ben-Arye, S., Harlev, M., Behlke, M., Benhar, I., Lieberman, J., Peer, D., 2018. A modular platform for targeted RNAi therapeutics. Nat. Nanotechnol. 13 (3), 214–219.

Kim, J., Eygeris, Y., Gupta, M., Sahay, G., 2021. Self-assembled mRNA vaccines. Adv. Drug Deliv. Rev. 170, 83–112.

Knop, K., Hoogenboom, R., Fischer, D., Schubert, U., 2010. Poly(ethylene glycol) in drug delivery: pros and cons as well as potential alternatives. Angew. Chem. Int. Ed. Engl. 49 (36), 6288–6308.

Kulkarni, J.A., Darjuan, M.M., Mercer, J.E., Chen, S., van der Meel, R., Thewalt, J.L., Tam, Y.Y.C., Cullis, P.R., 2018. On the Formation and Morphology of Lipid Nanoparticles Containing Ionizable Cationic Lipids and siRNA. ACS Nano 12 (5), 4787–4795.

Kumar, A., Erasquin, U.J., Qin, G., Li, K., Cai, C., 2010. "Clickable", polymerized liposomes as a versatile and stable platform for rapid optimization of their peripheral compositions. Chem. Commun. (Camb.) 46 (31), 5746. https://doi.org/10.1039/c0cc00784f.

Leal, M.P., Assali, M., Fernández, I., Khiar, N., 2011. Copper-catalyzed azide-alkyne cycloaddition in the synthesis of polydiacetylene: "click glycoliposome" as biosensors for the specific detection of lectins. Chemistry 17 (6), 1828–1836.

Lee, R.J., Low, P.S., 1995. Folate-mediated tumor cell targeting of liposome-entrapped doxorubicin in vitro. BBA 1233 (2), 134–144.

Leung, A.K.K., Hafez, I.M., Baoukina, S., Belliveau, N.M., Zhigaltsev, I.V., Afshinmanesh, E., Tieleman, D.P., Hansen, C.L., Hope, M.J., Cullis, P.R., 2012. Lipid Nanoparticles Containing siRNA Synthesized by Microfluidic Mixing Exhibit an Electron-Dense Nanostructured Core. J. Phys. Chem. C Nanomater Interf. 116 (34), 18440–18450.

Leung, A.K.K., Tam, Y.Y.C., Chen, S., Hafez, I.M., Cullis, P.R., 2015. Microfluidic Mixing: A General Method for Encapsulating Macromolecules in Lipid Nanoparticle Systems. J. Phys. Chem. B 119 (28), 8698–8706.

Lopes de Menezes, D.E., Pilarski, L.M., Allen, T.M., 1998. In vitro and in vivo targeting of immunoliposomal doxorubicin to human B-cell lymphoma. Cancer Res. 58, 3320–3330.

Luciani, A., Olivier, J.-C., Clement, O., Siauve, N., Brillet, P.-Y., Bessoud, B., Gazeau, F., Uchegbu, I.F., Kahn, E., Frija, G., Cuenod, C.A., 2004. Glucose-receptor MR imaging of tumors: study in mice with PEGylated paramagnetic niosomes. Radiology 231 (1), 135–142.

Mare, R., Paolino, D., Celia, C., Molinaro, R., Fresta, M., Cosco, D., 2018. Post-insertion parameters of PEG-derivatives in phosphocholine-liposomes. Int. J. Pharm. 552 (1-2), 414–421.

Moase, E.H., Qi, W., Ishida, T., Gabos, Z., Longenecker, B.M., Zimmermann, G.L., Ding, L., Krantz, M., Allen, T.M., 2001. Anti-MUC-1 immunoliposomal doxorubicin in the treatment of murine models of metastatic breast cancer. BBA 1510 (1-2), 43–55.

Mohanty, S., Jyotsana, N., Sharma, A., Kloos, A., Gabdoulline, R., Othman, B., Lai, C.K., Schottmann, R., Mandhania, M., Schmoellerl, J., Grebien, F., Ramsay, E., Thomas, A., Vornlocher, H.P., Ganser, A., Thol, F., Heuser, M., 2020. Targeted Inhibition of the NUP98-NSD1 Fusion Oncogene in Acute Myeloid Leukemia. Cancers (Basel) 12, 1–17.

Moreira, J.N., Ishida, T., Gaspar, R., Allen, T.M., 2002. Use of the post-insertion technique to insert peptide ligands into pre-formed stealth liposomes with retention of binding activity and cytotoxicity. Pharm. Res. 19, 265–269.

Nakamura, K., Yamashita, K., Itoh, Y., Yoshino, K., Nozawa, S., Kasukawa, H., 2012. Comparative studies of polyethylene glycol-modified liposomes prepared using different PEG-modification methods. BBA 1818 (11), 2801–2807.

Nakamura, T., Kawai, M., Sato, Y., Maeki, M., Tokeshi, M., Harashima, H., 2020. The Effect of Size and Charge of Lipid Nanoparticles Prepared by Microfluidic Mixing on Their Lymph Node Transitivity and Distribution. Mol. Pharm. 17 (3), 944–953.

Oude Blenke, E., Klaasse, G., Merten, H., Plückthun, A., Mastrobattista, E., Martin, N.I., 2015. Liposome functionalization with copper-free "click chemistry". J. Control. Release 202, 14–20.

Rothdiener, M., Müller, D., Castro, P.G., Scholz, A., Schwemmlein, M., Fey, G., Heidenreich, O., Kontermann, R.E., 2010. Targeted delivery of SiRNA to CD33-positive tumor cells with liposomal carrier systems. J. Control. Release 144 (2), 251–258.

Ryals, R.C., Patel, S., Acosta, C., McKinney, M., Pennesi, M.E., Sahay, G., 2020. The effects of PEGylation on LNP based mRNA delivery to the eye. PLoS One 15, e0241006.

Semple, S.C., Harasym, T.O., Clow, K.A., Ansell, S.M., Klimuk, S.K., Hope, M.J., 2005. Immunogenicity and rapid blood clearance of liposomes containing polyethylene glycol-lipid conjugates and nucleic acid. J. Pharmacol. Exp. Ther. 312 (3), 1020–1026.

Stefanetti, G., Allan, M., Usera, A., Micoli, F., 2020. Click chemistry compared to thiol chemistry for the synthesis of site-selective glycoconjugate vaccines using CRM197 as carrier protein. Glycoconj. J. 37 (5), 611–622.

Suk, J.S., Xu, Q., Kim, N., Hanes, J., Ensign, L.M., 2016. PEGylation as a strategy for improving nanoparticle-based drug and gene delivery. Adv. Drug Deliv. Rev. 99, 28–51.

Sun, S., Zou, H., Li, L., Liu, Q.i., Ding, N., Zeng, L., Li, H., Mao, S., 2019. CD123/CD33 dual-antibody modified liposomes effectively target acute myeloid leukemia cells and reduce antigen-negative escape. Int. J. Pharm. 568, 118518. https://doi.org/10.1016/j.ijpharm.2019.118518.

Takeuchi, I., Kanno, Y., Uchiro, H., Makino, K., 2019. Polyborane-encapsulated PEGylated Liposomes Prepared Using Post-insertion Technique for Boron Neutron Capture Therapy. J. Oleo Sci. 68 (12), 1261–1270.

Tseng, Y.-L., Hong, R.-L., Tao, M.-H., Chang, F.-H., 1999. Sterically stabilized anti-idiotype immunoliposomes improve the therapeutic efficacy of doxorubicin in a murine B-cell lymphoma model. Int. J. Cancer 80 (5), 723–730.

Uster, P.S., Allen, T.M., Daniel, B.E., Mendez, C.J., Newman, M.S., Zhu, G.Z., 1996. Insertion of poly(ethylene glycol) derivatized phospholipid into pre-formed liposomes results in prolonged in vivo circulation time. FEBS Lett. 386, 243–246.

van Moorsel, M.V.A., Urbanus, R.T., Verhoef, S., Koekman, C.A., Vink, M., Vermonden, T., Maas, C., Pasterkamp, G., Schiffelers, R.M., 2019. A head-to-head comparison of conjugation methods for VHHs: Random maleimide-thiol coupling versus controlled click chemistry. Int J Pharm X 1, 100020. https://doi.org/10.1016/j.ijpx.2019.100020.

Veiga, N., Goldsmith, M., Diesendruck, Y., Ramishetti, S., Rosenblum, D., Elinav, E., Behlke, M.A., Benhar, I., Peer, D., 2019. Leukocyte-specific siRNA delivery revealing IRF8 as a potential anti-inflammatory target. J. Control. Release 313, 33–41.

Veiga, N., Goldsmith, M., Granot, Y., Rosenblum, D., Dammes, N., Kedmi, R., Ramishetti, S., Peer, D., 2018. Cell specific delivery of modified mRNA expressing therapeutic proteins to leukocytes. Nat. Commun. 9, 4493.

Viger-Gravel, J., Schantz, A., Pinon, A.C., Rossini, A.J., Schantz, S., Emsley, L., 2018. Structure of Lipid Nanoparticles Containing siRNA or mRNA by Dynamic Nuclear Polarization-Enhanced NMR Spectroscopy. J. Phys. Chem. B 122 (7), 2073–2081.

Widmer, J., Thauvin, C., Mottas, I., Nguyen, V.N., Delie, F., Allémann, E., Bourquin, C., 2018. Polymer-based nanoparticles loaded with a TLR7 ligand to target the lymph node for immunostimulation. Int. J. Pharm. 535 (1-2), 444–451.

Witzigmann, D., Kulkarni, J.A., Leung, J., Chen, S., Cullis, P.R., van der Meel, R., 2020. Lipid nanoparticle technology for therapeutic gene regulation in the liver. Adv. Drug Deliv. Rev. 159, 344–363.

Yang, T., Choi, M.-K., Cui, F.-D., Kim, J.S., Chung, S.-J., Shim, C.-K., Kim, D.-D., 2007. Preparation and evaluation of paclitaxel-loaded PEGylated immunoliposome. J. Control. Release 120 (3), 169–177.